Materials Research. 2014; 17(3): 792-799
DOI: http://dx.doi.org/10.1590/S1516-14392014005000025

Characterization of the Complex Metal-clay Obtained in the Process of Lead Adsorption

M. G. A. Vieira[a]*, A. F. de Almeida Neto[a], M. L. Gimenes[b], M. G. C. da Silva[a]

[a]School of Chemical Engineering, Department of Design of Products and Processes, University of Campinas – UNICAMP, CEP 13083-852, Campinas, SP, Brazil
[b]Department of Chemical Engineering, University of Maringá – UEM, CEP 87020-900, Maringá, PR, Brazil

Received: December 5, 2013; Revised: January 22, 2014

This study aims to characterize the complex metal-clay formed by adsorption of lead. In this work, the bentonite clay named Fluidgel was calcined at 750 °C and was used as adsorbent for lead removal. The characterization of this clay and complex metal-clay was carried out by X-ray diffraction (XRD), Fourier transformer infrared spectroscopy (FTIR), surface area (BET method), scanning electron microscopy (SEM) and chemical composition by energy dispersive X-ray (EDX). The removal of lead from aqueous solution was carried out in a fixed bed. Dynamic experiments were performed to evaluate the effect of flowrate on adsorption efficiency. The experiments were accomplished at room temperature, the clay adsorbent particle diameter was of 0.855 mm and the flow rate varied from 0.6 to 2 mL/min. The feed concentration of lead was about 0.24 mmol/L. Comparing the chemical compositions of the clays obtained by EDX before and after removal of the lead, it was concluded that the ion exchange process might be important to lead removal. From the semi-quantitative analysis of chemical composition in clays with and without adsorbed lead it was observed a reduction of the amount of Ca^{2+}, K^{+} cations and the disappearance of Na^{+} cations, which was caused by cation exchange process.

Keywords: *characterization, complex metal-clay, lead, adsorption*

1. Introduction

The environmental impacts mainly originated by the constant discharge of all types of industrial pollutants by using water at some stage of the process reduce the self purifying ability of water. The pollutants present in water interferes with the metabolic cycles, due to the toxic effects they have on microorganisms. Particularly metals pollutants cause an increase in concentration of metals along the food chain (*biological amplification*), being one of the most problematic pollutants.

Metals have become a current and important topic both in environmental concerns and public health. Although some metals are essential for numerous metabolic processes, all metals are potentially toxic, carcinogenic and mutagenic if used excessively.

Traditional processes have been employed, along with new technologies, with the aim of contributing to the removal of metals present in the effluent wastewater[1]. Among various existing processes there are: ion exchange[2], the chemical precipitation[3] and ultrafiltration[4]. These methods are not always effective, and usuallyhave high cost and generate waste, thus, requiring a further stage of treatment.

Adsorption is one of the most effective and economical techniques used to remove metals present in wastewater[5], due to its simplicity when compared with other methods, such as ion exchange and precipitation. This method offers to the project flexibility with the possibility of conducting the metal removing operation in columns. This allows the treatment of large volumes of effluents continuously and under varied low concentration of metals present in feed, in addition to the high efficiency of contaminant removal that can be achieved.

Different adsorbents have been employed in the adsorption process: activated charcoal[6], ash[7-9], red mud[10], natural and synthetic zeolites[11], coffee husks[12], clays[13-17], vermiculite[18], among others.

The clays have properties such as high ion exchange capacity[19], they are easily available and offer a low cost alternative for metal removal[20], and are reusable[21]. In this context, this study aimed to evaluate the potential of an alternative adsorbent such as sodium bentonite clay, commercially called as Fluidgel, for the removal of Pb^{2+} present in aqueous effluents in dynamic system. The study focuses the adsorption of lead under dynamic conditions in a fixed bed column containing chemically and thermally treated (TACal) fluidigel. Evaluation of the behavior of breakthrough curves, kinetic data fitting to the Adams-Bohart model, investigation of removal cycles as well as the elution of lead from Fluidgel are presented in the paper.

2. Experimental

2.1. *Adsorbent material*

The Fluidigel clay was used as adsorbent after made by a heat treatment by calcination at 750 °C in muffle furnace and

*e-mail: melissagav@feq.unicamp.br

treated with acetic acid 4% in fixed bed. The heat treatment was realized in order to improve physical stability, and treatment with acetic acid was used towards to eliminate sodium carbonate in excess. This clay adsorbent was named Fluidgel TACal. The heat treatment provided a good stability and strength to the particles to be used in fixed bed column. The acid treatment was carried out to eliminate the excess of carbonate and hydroxyl present in the calcined Fluidgel. The calcined clay with an average particle diameter of 0.855 mm was packed inside the column and disposed in contact with deionized water for 2 hours. This washing process was performed before the treatment with acetic acid.

2.2. *Fixed bed column operations*

Sorption experiments under dynamic conditions were performed in a glass column (packed with Fluidigel TACal), jacketed with 1.5 cm internal diameter (ID) and 15 cm height. It was conducted several tests concerning monolithic lead removal having feed concentration of 0.24 mmol/L in this fixed bed column, being the curve of rupture obtained for flowrates of 0.6, 1, and 2 mL/min.. In order to evaluate the kinetic behavior of adsorption process of lead in fixed bed columns, the experimental data obtained were fitted to the Adams-Bohart model (*quasichemical)*[22].

The process efficiency was analyzed by calculating the mass transfer zone (MTZ), which, according to Geankoplis[23], is the fraction of the bed in which occurs the transfer of ionic species from the feed to the solid phase.

Useful quantities (q_u) and total (q_t) adsorbed in the bed until the break and saturation points, respectively, were calculated using a mass balance in the column. It was considered the breaking point, the moment in which the concentration of the solution leaving the bed was equivalent to 5% of the concentration at the entrance. The useful (q_u) and total (q_t) quantities removed, in mmol/g, can be calculated by Equations 1 and 2:

$$q_u = \frac{C_0 V}{m}\int_0^{t_b}\left(1-\frac{C|_{z=L}}{C_0}\right)dt \quad (1)$$

$$q_t = \frac{C_0 V}{m}\int_0^{\infty}\left(1-\frac{C|_{z=L}}{C_0}\right)dt \quad (2)$$

where C_0 is the lead initial concentration in the liquid phase in mmol/L, V is the volumetric flow of operation mL/min., t_b is the time which rupture occurs in the bed and m is the clay adsorbent mass in grams.

Geankoplis[23] presented a method to calculate the MTZ. The parameter $\delta=q_u/q_t$ refers to the fraction of the usable length of the bed to the breaking point. The usable length (H_u) and MTZ are calculated by Equations 3 and 4:

$$H_u = \delta.H_t \quad (3)$$

$$H_t = H_u + MTZ \quad (4)$$

where H_t is the column total length.

The Adams-Bohart model (*quasichemical*)[22] was used in the adjustment of kinetic behavior of data of lead adsorption process in fixed bed columns, according to Equation 5.

$$\frac{C}{C_0} = \frac{e^{\tau}}{e^{\tau}+e^{\xi}-1} \quad (5)$$

being, $\tau = kC_0\left(t-\frac{z}{v}\right)$, $\xi = \frac{kq_0 z}{v}\left(\frac{1-\varepsilon_L}{\varepsilon_L}\right)$, z the bed height, *v* is the velocity flow, ε_L the bed porosity and *t* is the time.

2.3. *Desorption tests*

Three experimental were performed to obtain the lead rupture curves using a solution of $CaCl_2$ 0.1 mol/L as eluent. In these experiments the eluent was pumped throughout the Fluidigel TACal packed column at the same flowrate (i.e.1mL/min.). The $CaCl_2$ was chosen from preliminary batch elution tests, in which were tested NaCl, disodium EDTA, HCl, Thiourea and $CaCl_2$. The $CaCl_2$ was the eluent that presented higher lead elution.

The amount of eluted lead, q_{el}, was calculated by integrating the elution curve. The area under this curve multiplied by the feeding flowrate, *V* (in mL/min.), per mass of calcined clay, *m* (in grams), gives the amount of eluted metal according to the Equation 6[24]. The elution percentage was determined by considering the total amount of lead previously adsorbed as 100% of eluted lead.

$$q_{el} = \frac{V}{m}\int C_{el}.dt \quad (6)$$

where C_{el} is the metal concentration in the liquid phase in mmol/L.

2.4. *Characterization*

The physical–chemical characterization of Fluidgel clay involved the following techniques: chemical analysis by energy dispersive X-ray spectroscopy (EDX) to identify and quantify the total chemical composition; The surface area was verified by physisorption of N_2 (BET method); The real density measured by helium picnometry; Morphological analysis by scanning electron microscopy (SEM), Identification of particular clay peaks and maintenance of its properties by X-ray diffraction (XRD), and Fourier transformer infrared spectroscopy (FTIR). The above mentioned analyses were performed for samples of commercial Fluidgel clay, calcined Fluidigel TACal before and after lead adsorption.

3. Results and Discussion

3.1. *Mass transfer effect*

The different behaviors of the breakthrough curves obtained at different flowrates (Figure 1) indicate the strong influence of the flow on diffusional resistances. The adsorption process for 0.6 mL/min. flowrate presented a strong resistance to saturation of the bed, confirmed by the more elongate breakthrough curve.

In Table 1 the useful (q_u) and total (q_t) quantities of metal retained in the bed were obtained considering the outlet bed concentrations equal to 5 and 95% of the entrance concentration, respectively.

It can be observed (Table 1) that for the flowrate of 1 mL/min. a relative low value of MTZ length (3.4 cm) as well as a low resistance to mass transfer, observed by the jump in the curve after the breakthrough point (Figure 1) for lead removal by the clay, in addition to the greater percentage removal (47.03%). For this reason the flowrate selected to be used in other experiments of lead removal with Fluidgel TACal was 1 ml/min.

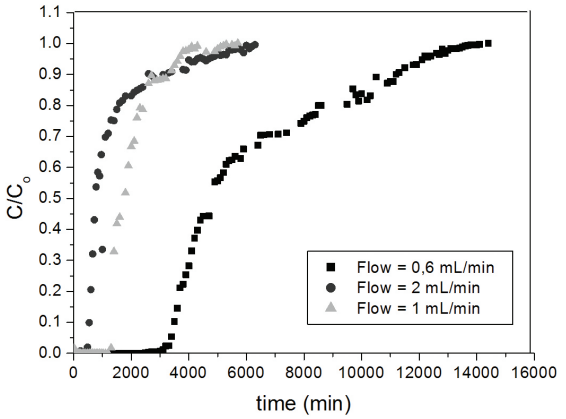

Figure 1. Breakthrough curves for the system of Pb^{2+}/calcined Fluidgel for different flow, particle size = 0.855 mm and C_0 = 0.24 mmol/L.

The Adams-Bohart model parameters: constant velocity of adsorption linear (K), and the maximum quantity of adsorbate adsorbed by bed volume (q_0) for each flowrate are listed in Table 2. Results concerning the fitting of the Adams-Bohart model are presented in Figure 2.

The model did not fit experimental data for the lowest flowrate (0.6 mL/min.) In spite of this, the results in Table 2 shows that with the increase of the flowrate, the constant kinetics increases, which shows that with higher linear adsorption rate, a smaller amount of lead will be retained by this clay.

3.2. *Beds regeneration*

The breakthrough curves obtained with experiments envolving adsorption/desorption cycles, being the adsorvent regenerated using as eluent $CaCl_2$ 0.1 mol/L are shown in Figure 3a.

According to the results, there are different behaviors of the breakthrough curves for the three cycles, in which

Table 1. MTZ, q_u, q_t and $\%R_L$ for lead removal on Fluidgel TACal.

System	Flow (mL/min.)	MTZ (cm)	q_u (mmol/g)	q_t (mmol/g)	%Rem
Pb/Fluidgel TACal	0.6	0.425	0.0165	0.016	27.91
	1	3.413	0.0139	0.018	47.03
	2	7.839	0.0102	0.020	21.35

Table 2. Fitting parameters of the Adams-Bohart model to study flow.

System	Flow (mL/min.)	k (L/mmol.min)	q_0 (mmol/L)	R^2
Pb/Fluidgel TACal	0.6	-	-	-
	1.0	0.0125	36.2	0.9918
	2.0	0.0147	19.02	0.9773

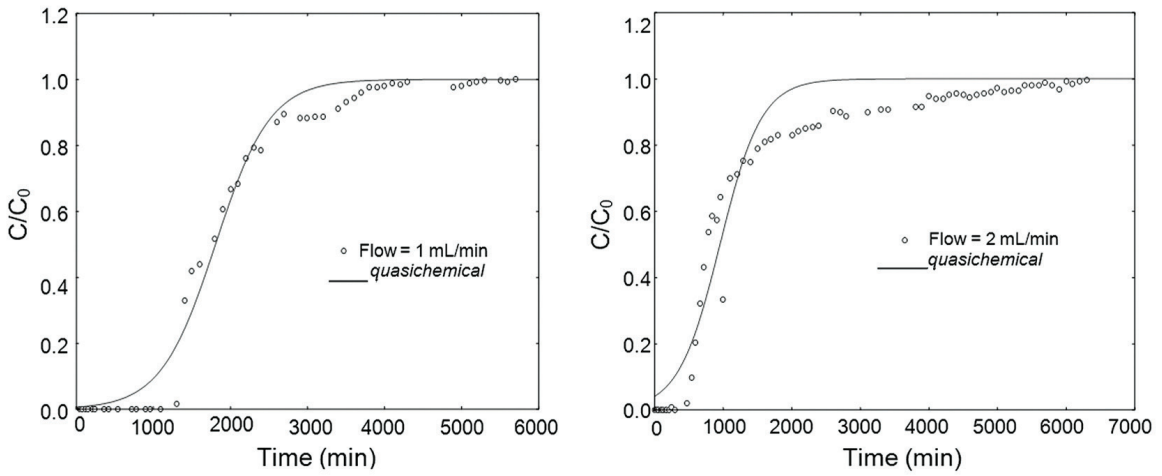

Figure 2. Adams – Bohart adjustments to the curves of Pb^{2+} removal by Fluidgel TACal at different flows.

it can be observed that the greater mass transfer resistance has been obtained in the last cycle with a low removal. The breakthrough time (t_b) remained around 800 min. for the first two cycles. Table 3 summarizes the total and the useful quantities removed, the MTZ and the percentage removal for Pb^{2+}/Fluidigel TACal clay.

The lead removal obtained up to bed saturation in the first cycle, was 0.0378 mmol/g, decreasing in the second and third cycles (0.0248 and 0.0206 mmol/g). The curves of the Figure 3a showed different behaviors, indicating the influence of chemical modification in diffusional resistances.

The breakthrough curve for the second cycle of the bed showed a behavior that approaches it to a step function, suggesting a low diffusional resistance compared to the first cycle, obtaining a more favorable removal process. This result indicates that, due to the passage of the eluent, all the exchange sites were located in an area readily accessible to lead ions. Whereas, in the first cycle the breakthrough curves showed weaker inclination rupture, a higher diffusional resistances characteristic. This result indicates that all exchange sites were located on a more intrinsic surface.

In the third cycle, there is a decrease in useful quantities and total removed, and percentage removal, related to the strong stability between the complex of the metal and the clay after two cycles of adsorption. The desorption process through eluting occurs, predominantly, in the first two hours of contact, in which almost all lead is eluated (Figure 3b). Table 4 presents the variables responses of the regeneration of the bed by $CaCl_2$ for Fluidgel TACal.

The solvent recovery efficiency (SRS) can be evaluated by the ratio of the volume of water spent in the preparation of eluents (V_E) corresponding to the elution time and the volume of purified water (V_b) to the breakthrough point, considering that the eluent has concentrated all lead in the clay after saturation of the bed. Based on breakthrough time and elution time, the volumes V_b and V_E and SRS were calculated and are presented in Table 5. According to Table 5, most SRS was presented for the first elution, because the second was used more volume of eluent for desorption. After the third adsorption the bed became unstable, with great loss of load, preventing the third elution.

For each of the breakthrough curve the Adams-Bohart model curve (*quasichemical*) was fitted to the experimental data, as shown in Figure 4. The values of coefficients adjusted are shown in Table 6. It can be observed that the parameter k varies according each clays elution test, meaning that after each elution a new kinetics is established.

3.3. *Adsorbent characterization*

From the semiquantitative analysis of chemical composition showed in Table 7, it can be observed that with the lead adsorption, there was a reduction of the amount of

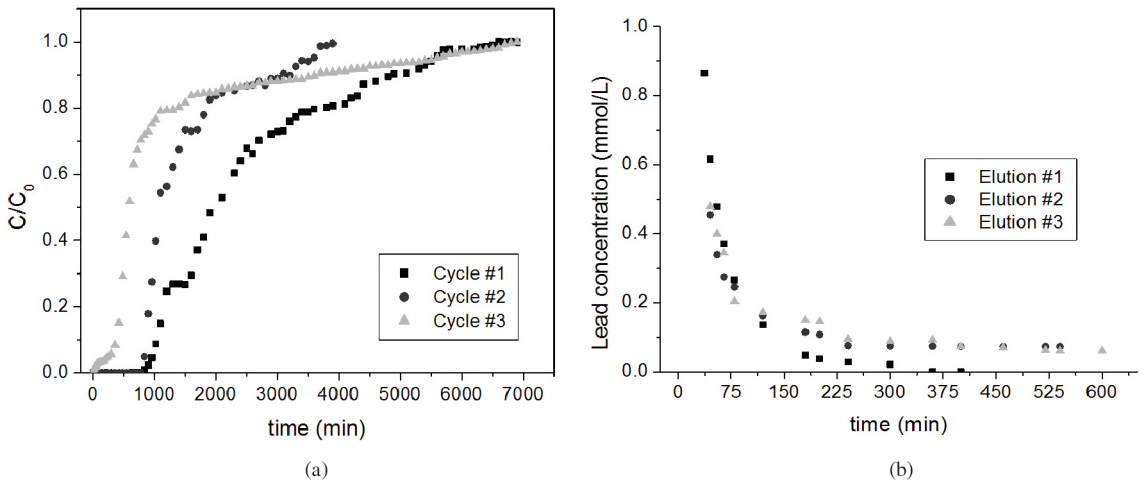

(a) (b)

Figure 3. (a) Adsorption and (b) desorption curves for the system of Pb^{2+}/calcined Fluidgel (flow = 1 mL/min., particle size = 0.855 mm, C_0 = 0.36 mmol/L).

Table 3. Parameters of breakthrough curves for the removal of lead in adsorption/desorption cycles using $CaCl_2$ (0.1 mol/L) as eluent.

System	Cycle #	MTZ (cm)	q_u (mmol/g)	q_t (mmol/g)	%Rem
Pb/Fluidgel TACal	1	7.849	0.0176	0.0378	37.91
	2	5.627	0.0155	0.0248	38.42
	3	10.39	0.0063	0.0206	20.51

Table 4. Parameters regeneration of the columns with $CaCl_2$ 0.1 mol/L.

System	Eluition #	elution time (min)	q_{el} (mmol/g)	Eluition %	Error (%)
Pb/Fluidgel TACal	1	400	0.0416	100	10.04
	2	550	0.0269	100	8.434
	3	600	0.0236	100	14.51

Table 5. Balance recovered water removal - elution of lead.

System	Eluition #	t_b (min)	V_b (mL)	t eluition (min)	V_E (mL)	SRS (%)
Fluidgel TACal/Pb	1	817.64	817.64	400	400	51.07
	2	813.13	813.13	550	550	32.36

Table 6. Fitting parameters of Adams-Bohart model for breakthrough curves in beds regenerated by $CaCl_2$.

System	Removal #	k (L/mmol.min)	q_0 (mmol/L)	R^2
Pb/Fluidgel TACal	1	0.0382	75.38	0.9865
	2	0.0297	41.03	0.9788
	3	0.0198	24.26	-

Table 7. Chemical composition by EDX.

Sample	Composition (%)									
	Na	Mg	Al	Si	K	Ca	Ti	Fe	Pb	Cd
Fluidgel TACal	3.07	3.52	15.30	64.20	0.54	2.70	1.06	9.57	0	0
Fluidgel TACal +Pb	0.12	4.59	13.74	62.52	0.29	1.47	1.02	13.04	2.84	0

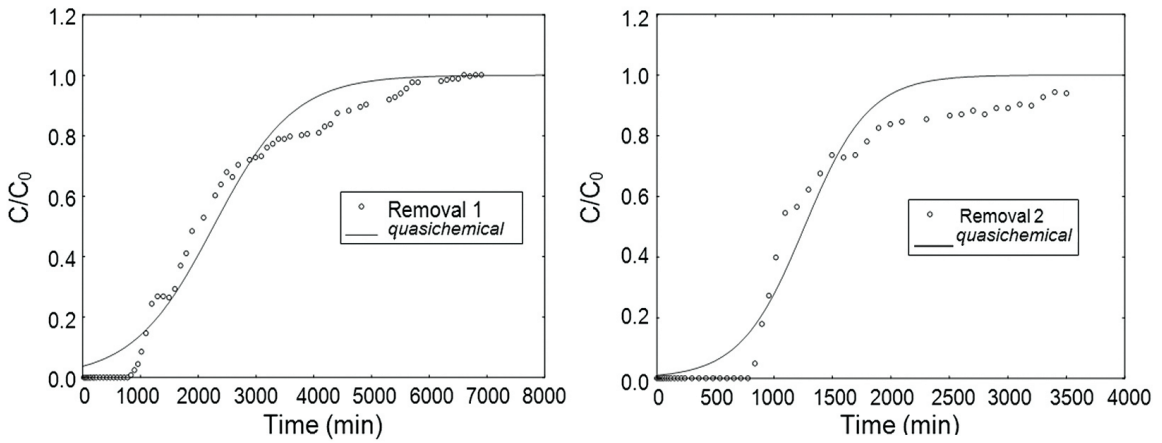

Figure 4. Fitting of the Adams – Bohart model of beds regenerated by $CaCl_2$.

cations Ca^{2+} and $K^+$and almost disappearance of cations Na^+. This emphasizes the occurrence of cation exchange in the process of lead removal by the Fluidgel TACal.

The XRD analyses for clay samples of Fluidgel TACal, before and after lead adsorption, are shown in Figure 5. In each diffractogram, for the considered band, there are two characteristic peaks for montmorillonite and the others are related to quartz. It can be observed that the Fluidgel clay samples analyzed are not characterized by a highly crystalline structure, as it is found, for example, in zeolites, since the peaks detected in these samples are well defined. The difficulty in identifying peaks is explained by nondiffraction of X-ray, which had a deviation throughout the process, what could characterize the formation of an inter-crystalline joint of clays.

Through the diffractograms, there is a significant deviation of the particular montmorillonite peak (Fluidgel TACal) ($2\theta = 8.69°$) for an angle 2θ higher (9.4°) obtained for the other sample, which indicates shorter plane interlayer distances (d_{001}), besides a reduction in the peaks intensity in the region of Fluidgel TACal clay with adsorbed lead, in relation to the Fluidgel TACal clay without this metal.

From BET analysis, there was a negligible small increase in the surface area of the adsorbent after the removal process from 11 to 13 m^2/g, which could be possibly due to lead adsorption. The real density reduction after lead removal, from 2.5 to 2.3 g/cm^3 is caused by material losses during the process.

The morphologic analysis of Fluidgel TACal clay particles by scanning electron microscopy provided the micrograph shown in Figure 6, whose dots indicate the mapping of the adsorbed lead on Fluidgel TACal. It can be noticed a homogeneous distribution of the adsorbed lead throughout the whole surface of the clay Fluidigel TACal particle.

The FTIR spectra for plain sample of Fluidgel TACal and sample with adsorbed lead are shown in Figure 7. According to these spectra, the band figures that correspond to the OH–stretching remain the same in both samples, in spite of a small deviation in band positions. The band

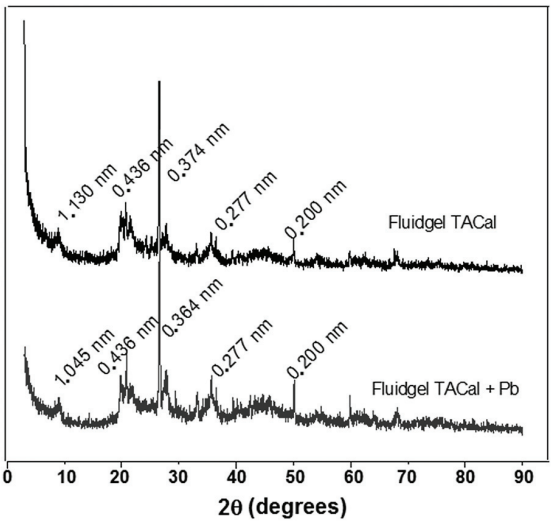

Figure 5. Diffractogram of Fluidgel TACal and Fluidgel TACal + Pb adsorbed.

in 783-797 cm^{-1} originated by the existence of quartz in Fluidgel clay did not practically change position after lead adsorbed. According to the FTIR spectra for clay sample contain lead, no bending band for metal–oxygen bond was observed. Consequently, it may be concluded that lead removal by Fluidge TACal clay was mainly caused by ion exchange between the structures that contain clay tetrahedral and octahedral layers in the clay.

4. Conclusions

The study of the mass transfer parameters, as well as the breakthrough curves, indicate that the most suitable flow ratio was 1 mL/min., with a low value of MTZ length (3.4 cm), and a low resistance to mass transfer for lead removal by Fluidgel TACal. According to the results of the adsorption/desorption, different behaviors of the breakthrough curves for the three cycles, suggest that regeneration of the bed causes changes in the clay reducing its adsorption capacity. The breakthrough time (t_b) remained around 800 min. for the first two cycles. The coefficients

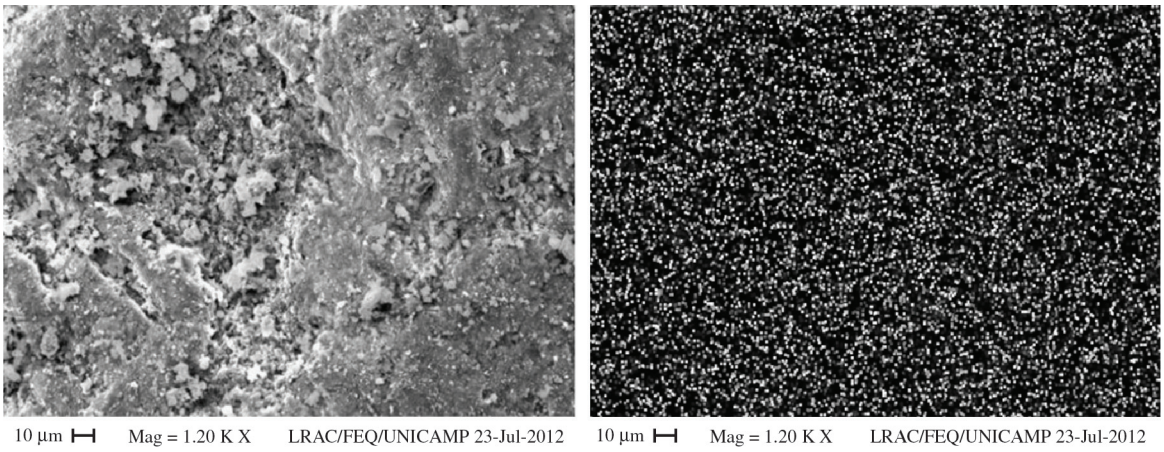

Figure 6. Metal mapping on Fluidgel TACal clay (dp = 0.855 mm) with 1200×amplified. The dots in micrograph right represent adsorbed lead on Fluidgel TACal.

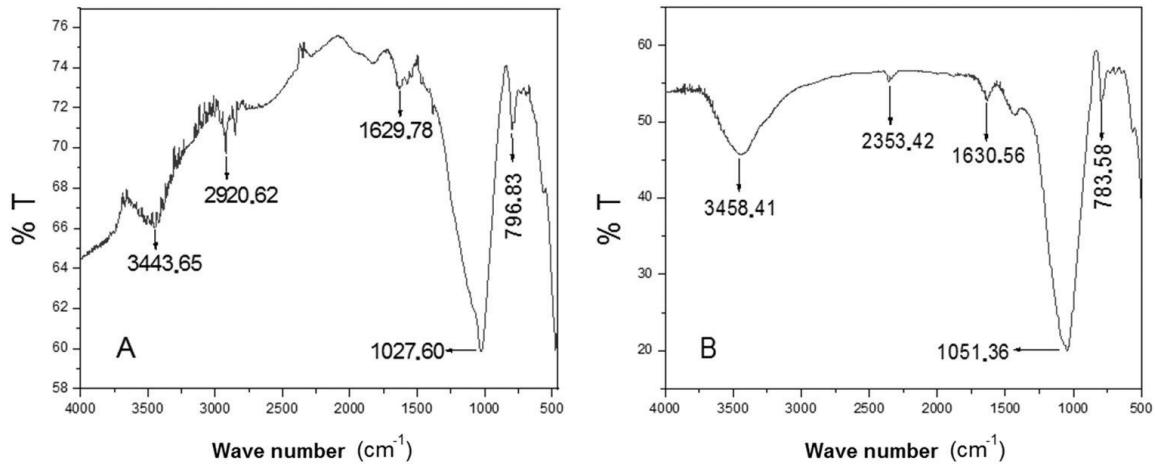

Figure 7. Spectra for FTIR of (a) Fluidgel TACal and (b) Fluidgel TACal + Pb.

parameters of adjustment of the Adams-Bohart model in regenerated beds indicate that the parameter k varies with each elution test and this can be explained because after elution a new kinetics is established. Based on the physical and chemical analysis of Fluidgel TACal clay, it can be considered poly-cationic material, but not characterized by highly crystalline structure. The adsorption spectra in the infrared region showed adsorption bands corresponding to the OH–stretching band, as well as the presence of quartz in clay. Metal–oxygen stretching vibrations in the octahedral and tetrahedral regions were not found. These conclusions combined with the results of the semiquantitative analysis of chemical composition give clear evidence of ion exchange in the lead removal process occurring in the interlayer clay structures.

Acknowledgements

The authors would like to thank FAPESP (São Paulo Research Foundation) for financial support.

References

1. Bayhan YK, Keskinler B, Cakici A, Levent M and Akay G. Removal of divalent heavy metal mixtures from water by *Saccharomyces cerevisiae* using cross-flow micro-filtration. *Water Research*. 2001; 35(9):2191-2200. http://dx.doi.org/10.1016/S0043-1354(00)00499-1
2. Shaidan NH, Eldemerdash U and Awad S. Removal of Ni(II) ions from aqueous solutions using fixed-bed ion exchange column technique. *Journal of the Taiwan Institute Chemical Engineers*. 2012; 43(1):40-45. http://dx.doi.org/10.1016/j.jtice.2011.06.006
3. Chen Q, Luo Z, Hills C, Xue G and Tyrer M. Precipitation of heavy metals from wastewater using simulated flue gas: Sequent additions of fly ash, lime and carbon dioxide. *Water Research*. 2009; 43(10):2605-2614. http://dx.doi.org/10.1016/j.watres.2009.03.007
4. Landaburu-Aguirre J, García V, Pongrácz E and Keiski RL. The removal of zinc from synthetic wastewaters by micellar-enhanced ultrafiltration: statistical design of experiments. *Desalination*. 2009; 240(1-3):262-269. http://dx.doi.org/10.1016/j.desal.2007.11.077
5. Tran HH, Roddick FA and O'Donnell JA. Comparison of chromatography and desiccant silica gels for the adsorption of metal ions—I. adsorption and kinetics. *Water Research*. 1999; 33(13):2992-3000. http://dx.doi.org/10.1016/S0043-1354(99)00017-2
6. Yanagisawa H and Matsumoto Y and Machida M. Adsorption of Zn(II) and Cd(II) ions onto magnesium and activated carbon composite in aqueous solution. *Applied Surface Science*. 2010; 256(6):1619-1623. http://dx.doi.org/10.1016/j.apsusc.2009.10.010
7. Vieira MGA, Almeida Neto AF, Da Silva MGC, Nóbrega CC and Melo AA Fº. Characterization and use of in natura and calcined rice husks for biosorption of heavy metals ions from aqueous effluents. *Brazilian Journal of Chemical Engineering*. 2012; 29(3):619-633. http://dx.doi.org/10.1590/S0104-66322012000300019
8. Vieira MGA, Almeida Neto AF, Da Silva MGC, Nóbrega CC and Melo AA Fº. Influence of the system on adsorption of Pb(II) and Cu(II) by calcined rice husks: kinetic study. *Chemical Engineering Transactions*. 2011; 24:1213-1218.
9. Gupta VK, Jain CK, Ali I, Sharma M and Saini VK. Removal of cadmium and nickel from wastewater using bagasse fly ash—a sugar industry waste. *Water Research*. 2003; 37(16):4038-4044. http://dx.doi.org/10.1016/S0043-1354(03)00292-6
10. Nadaroglu AH, Kalkanb E, Demir N. Removal of copper from aqueous solution using red mud. *Desalination*. 2010; 251(1-3):90-95. http://dx.doi.org/10.1016/j.desal.2009.09.138
11. Apiratikul R and Pavasant P. Sorption of Cu^{2+}, Cd^{2+}, and Pb^{2+} using modified zeolite from coal fly ash. *Chemical Engineering Journal*. 2008; 144(2):245-258. http://dx.doi.org/10.1016/j.cej.2008.01.038
12. Oliveira L, Franca AS, Alves TM and Rocha SDF. Evaluation of untreated coffee husks as potential biosorbents for treatment of dye contaminated waters. *Journal of Hazardous Materials*. 2008; 155(3):507-512. http://dx.doi.org/10.1016/j.jhazmat.2007.11.093
13. Galindo LSG, Almeida Neto AF, Da Silva MGC and Vieira MGA. Removal of cadmium(II) and lead(II) ions from aqueous phase on sodic bentonite. *Materials Research*. 2013; 16(2):515-527. http://dx.doi.org/10.1590/S1516-14392013005000007
14. Almeida Neto AF, Vieira MGA and Silva MGC. Cu(II) adsorption on modified bentonitic clays: different isotherm behaviors in static and dynamic systems. *Materials Research*. 2012; 15(1):114-124. http://dx.doi.org/10.1590/S1516-14392011005000089
15. Vieira MGA, Almeida Neto AF, Gimenes ML and Da Silva MGC. Removal of nickel on Bofe bentonite calcined clay in porous bed. *Journal of Hazardous Materials*. 2010A; 176(1-3):109-118. http://dx.doi.org/10.1016/j.jhazmat.2009.10.128
16. Vieira MGA, Almeida Neto AF, Gimenes ML and Da Silva MGC. Sorption kinetics and equilibrium for the removal of nickel ions from aqueous phase on calcined Bofe bentonite clay. *Journal of Hazardous Materials*. 2010B; 177(1-3):362-371. http://dx.doi.org/10.1016/j.jhazmat.2009.12.040
17. Kubilay S, Gürkan R, Savran A and Sahan T. Removal of Cu(II), Zn(II) and Co(II) ions from aqueous solutions by adsorption onto natural bentonite. *Adsorption*. 2007; 13(1):41-51. http://dx.doi.org/10.1007/s10450-007-9003-y
18. Nishikawa E, Almeida Neto AF and Vieira MGA. Equilibrium and thermodynamic studies of zinc adsorption on expanded vermiculite. *Adsorption Science and Technology*. 2012; 30(8/9):759-772. http://dx.doi.org/10.1260/0263-6174.30.8-9.759
19. Meier LP and Kahr G. Determination of the cation exchange capacity (cec) of clay minerals using the complexes of copper(ii) ion with triethylenetetramine and tetraethylenepentamine. *Clays and Clay Minerals*. 1999; 47:386-388. http://dx.doi.org/10.1346/CCMN.1999.0470315
20. Bailey SE, Olin TJ, Bricka M and Adrian D. A review of potentially low-cost sorbents for heavy metals. *Water Research*. 1999; 33:2469-2479. http://dx.doi.org/10.1016/S0043-1354(98)00475-8
21. Gimenes ML, Almeida Neto AF, Vieira MGA and Silva MGC. Continuous-flow copper adsorption in regenerable calcined clay columns. *Chemical Engineering Transactions*. 2013; 32:2023-2028.
22. Ruthven DM. *Principals of Adsorption and Adsorption Processes*. John Wiley & Sons; 1984.
23. Geankoplis CJ. *Transport Processes and Unit Operations*. 3rd ed. PTR Prentice Hall; 1993.
24. Volesky B, Weber J and Park JM. Continuous-flow metal biosorption in a regenerable Sargassum column. *Water Research*. 2003; 37(2):297-306. http://dx.doi.org/10.1016/S0043-1354(02)00282-8

Nomenclature

C_0: metal initial concentration in the liquid phase, (mg/L);
$C|_{z=L}$: metal concentration in solution at the column exit, (mg/L);
H_t: height of the bed (cm);
H_u: usable length of the bed (cm);
m: dry mass of adsorbent (g clay);
q_t: total adsorption capacity of the metal (mg metal/ g of clay);
q_u: quantity of adsorbed metal per unit of adsorbent mass after the breakthrough point, (mg metal/g of adsorbent);
t_b: time until the breaking point (min);
t_{tot}: time for the total removal, (min);
t: time (min);
V: volume outflow (cm_3/min);
z: the bed height (cm);
v: velocity flow (cm/min);
ε_L: bed porosity.